2.7. In vivo gene delivery study

For measuring the knockdown efficiency of Tie2 or FVII gene expression by YSK05-MEND modified with different mol% of KLGR-PEG or STR-KLGR or STR-R8, the male ICR mice were injected intravenously with either Tie2 siRNA or FVII siRNA encapsulated modified or unmodified YSK05-MEND at a siRNA dose of 1 mg/kg of body weight. After 24 h of incubation, the mice were sacrificed and livers, lung or kidneys were collected.

2.8. RNA extraction and PCR analysis

RNA was extracted from mouse tissue (liver, lung and kidney) using TRIzol reagent (Invitrogen Inc.). According to the manufacturer's instructions, complementary DNA (cDNA) was prepared from 1 μg of RNA samples using the high capacity RNA-to-cDNA Kit (ABI). The resulting cDNA was diluted, and a 5 μl of solutions was used in a 20 μl PCR reaction (SYBR Green; TOYOBO) containing the specific primers. Duplicate PCR reactions were run for each samples and quantification of each samples were performed using the Mx3005P Real-time QPCR system (Agilent). Cycle threshold (Ct) values were normalized to beta-actin expression, and results were expressed as the fold change in mRNA compared with control mice.

2.9. Confocal microscopy experiment

ICR mice were given an intravenous injection of rhodamine labeled STR-KLGR modified MEND and the mice were killed 25 min after the treatment. The portal vein was cut and a needle was introduced into the vena cava and 10–15 ml of heparin containing a PBS (40 units/ml) solution was used to remove the remaining blood and cell surface bound MEND in the liver. The liver was then excised and washed with saline and sliced into 10–15 mm-sized blocks with scissors. Liver sections were then incubated with a 20 fold volume of a diluted solution of Hoechst 33342 (1 mg/ml) and Isolectin B4 in HEPES buffer for 1 h. The specimens were placed on a 35 mm glass base dish (IWAKI, Osaka, Japan) and observed by confocal laser scanning microscopy (A1Confocal Laser Microscope System, Nikon Instruments Inc., Tokyo, Japan).

2.10. In vitro quantitative cellular uptake study

The quantitative measurement of cellular uptake of the STR-KLGR modified MEND was determined by flow cytometry. Empty MENDs modified with or without STR-KLGR at different mol% were prepared as described in Section 2.5. The MENDs were labeled with NBD-DOPE. Primary LSECs were seeded at a density of 200,000 cells per well in a 6-well plate with medium. After 24 h of seeding period, the cells were incubated with MENDs in serum free medium for 1 h. The cells were then washed with PBS (−) supplemented with a heparin solution (20 unit/ml). Trypsin was then added to each well and each sample was collected in a different eppendorf tube by centrifugation (3000 rpm, 4 °C, for 3 min). Cell pellets were resuspended in 1 ml of PBS (−) supplemented with 0.5% BSA and 0.1% NaN_3 (FACS buffer). To remove aggregated cell and debries, the cells were filtered through a nylon mesh. Then the filtered cells were analyzed by flow cytometry (FACScan, Becton Dickinson). The cellular uptake of NBD-DOPE labeled MEND was expressed as the mean fluorescence intensity, calculated using the CellQuest software (Becton Dickinson).

2.11. Endosomal escape efficiency of STR-KLGR modified MEND

100,000 LSECs were seeded on a 35 mm glass-base dish (IWAKI, Osaka, Japan) in 2 ml of EBM-2 medium containing serum and other essential factors. At 24 h after the seeding, the culture medium was removed and the cells were washed with 1 ml of serum-free medium. Then the cells were incubated with cy3 labeled siRNA loaded MEND either modified or unmodified with STR-KLGR. Then after 30 min of incubation at 37 °C, Lysotracker green was added to the cell dish to stain endosomal/lysosomal compartment. Then after 45 min of incubation, Hoechst 33342 was added to stain the cell nucleus. Then after a total of 1 h, the incubation medium was washed with PBS supplemented with heparin (20 units/ml) for 3 times. The cells were then suspended in Kreb's buffer and confocal images were obtained by confocal laser scanning microscopy (A1Confocal Laser Microscope System, Nikon Instruments Inc., Tokyo, Japan). Minimum 6–8 pictures were taken where there were minimum 2–3 cells in each image with CFI Apochromat TIRF 60× oil, NA1.49 lens. Then each image was transferred to Scope-Pro 7.0 configuration software to quantify the pixel areas in each cell separately. For every sample, total 10 cells were analyzed.

2.12. Uptake mechanism study

For the investigation of mechanism of cellular uptake of the STR-KLGR modified MEND, 200,000 primary LSECs or Hepa1–6 cells were seeded on a 35 mm glass-base dish (IWAKI, Osaka, Japan) in 2 ml of EBM-2medium supplemented with serum and other essential factors for 24 h. At the day of the experiment, the cells were washed with 1 ml PBS. Then the dishes were pre-incubated with serum-free medium in the absence or presence of inhibitor. The following inhibitors were added separately in separate dishes and incubated for different time schedule: amiloride (5 mM) for 30 min, filipin (150 μg/ml) for 45 min and sucrose (0.5 M) for 30 min. Then after the mentioned incubation time 50 nM of STR-KLGR modified or unmodified MEND encapsulating cy3 labeled Tie2 siRNA was added and the cells were incubated with or without inhibitor for another 1 h. Nuclei were stained with Hoechst 33342 for 10 min before washing. The cells were then washed with 1 ml of ice-cold PBS supplemented with heparin (20 units/ml) for 3 times to completely wash the surface bound MEND. The cells were then kept on ice in 2 ml of Kreb's buffer and images were taken by confocal microscopy. A brief result of this experiment has been summarized in Table 2.

2.13. Toxicological study

For toxicological studies, 4-week-old male ICR mice were injected intravenously with the STR-KLGR modified YSK05-MEND encapsulating Tie2 siRNA at a siRNA dose of 1 mg/kg body weight. After 24 h, blood samples were collected by cutting the tail vein and serum levels of AST and ALT were then measured using a colorimetric diagnostic kit (Wako Pure Chemical Industries Ltd.) according to the manufacturers guidelines.

2.14. Statistical analysis

Comparisons between multiple treatments were made using one-way analysis of variance (ANOVA), followed by the 'Dunnett test'. Pair-wise comparisons of subgroups were made using the Student's *t*-test. Differences among the means were considered to be statistically significant at a *p*-value of <0.05 and <0.01.

3. Results

3.1. The characteristics of KLGR-PEG or STR-KLGR modified YSK05-MEND

The YSK05-MEND was modified with different mol% of KLGR-PEG or STR-KLGR. The physical properties of the prepared MENDs are shown in Table 1. Particle size of the MEND and zeta-potentials

Table 1
Physical characteristics of YSK05-MEND.

Sample	KLGR-PEG$_{2000}$-YSK05-MEND		STR-KLGR-YSK05-MEND	
	Size (nm)	Zeta potential (mV)	Size (nm)	Zeta potential (mV)
YSK05-MEND$_{0\%KLGR}$	84 ± 3	6.1 ± 0.4	–	–
YSK05-MEND$_{1\%KLGR}$	86 ± 2	12.2 ± 0.6	90 ± 1	8.1 ± 0.9
YSK05-MEND$_{3\%KLGR}$	84 ± 3	18.1 ± 0.4	81 ± 2	19.1 ± 1.5
YSK05-MEND$_{5\%KLGR}$	118 ± 3	21.9 ± 2.8	103 ± 2	25.7 ± 0.5

were measured by a Malvern Zetasizer. Average diameter of the YSK05-MEND was within the range of 80–120 nm. The addition of a ligand at the MEND surface did not significantly affect particle size until the concentration of STR-KLGR or KLGR-PEG at the surface of MEND reached to 5 mol%. The surface charge of the unmodified YSK05-MEND was nearly neutral (6 mV), while the addition of the KLGR-PEG or STR-KLGR increased the surface charge with the increasing ligand density at the MEND surface. The surface charge of the modified YSK05-MEND was within the range of 8–25 mV. The percentage of siRNA encapsulation was measured by means of a RiboGreen assay which showed that the siRNA encapsulation efficiency ranged from 75 to 90%.

3.2. In vivo gene silencing activity of KLGR-PEG or STR-KLGR modified YSK05-MEND

An in vivo gene expression knockdown experiment was performed to evaluate the capacity for delivering the siRNA contained by our developed carrier to LSEC. For the measurement of knockdown efficiency of Tie2 gene expression, an endothelial cell specific marker, Tie2 siRNA was delivered through a KLGR-PEG or STR-KLGR modified YSK05-MEND. As shown in Fig. 1, the KLGR-PEG modified YSK05-MEND failed to show a significant knockdown of gene expression while, in the case of STR-KLGR, the maximum knockdown of the Tie2 gene was observed when the ligand density at the MEND surface was 1 mol%. In addition the gene expression was increased with increasing mol% of STR-KLGR at the MEND surface. From these data, it is clear that although the ligand density at the surface of MEND was increased, the knockdown of gene expression was decreased.

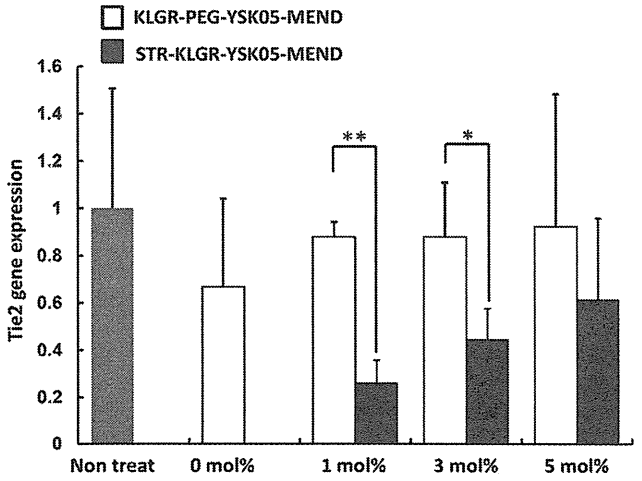

Fig. 1. In vivo Tie2 gene expression by the YSK05-MEND modified with different mol% of KLGR-PEG or STR-KLGR. Male ICR mice were intravenously injected with YSK05-MEND modified with different mol% of KLGR-PEG or STR-KLGR encapsulating Tie2 siRNA in the core. Liver samples were collected after 24 h of incubation. After collecting mRNA from liver samples, Tie2 gene expression level was measured by RT-PCR. Number of mouse in each sample group = 6. Statistical analysis within each groups was done by unpaired *t*-test, where $^{**}P < 0.01$ and $^{*}P < 0.05$.

3.3. In vivo accumulation of STR-KLGR modified YSK05-MEND in the liver

As in Section 3.2, the knockdown of gene expression was not increased with an increase in the mol% of ligand at the surface of YSK05-MEND. Therefore, we were prompted to perform an in vivo accumulation study of the developed nanocarrier in the liver by confocal microscopy. The pattern of accumulation of the STR-KLGR modified YSK05-MEND showed that the uptake of the modified MEND increased with increasing ligand density at the surface of the MEND (Fig. 2). The rhodamin-DOPE labeled YSK05-MEND merges with isolectin B4 stained blood vessels, which indicates that the MEND accumulated through the blood vessels.

3.4. Cellular uptake by flow cytometry

To support the in vivo uptake results for the YSK05-MEND modified with different mol% of STR-KLGR, we measured an in vitro uptake by flow cytometry. In this experiment (Fig. 3), the cellular uptake of STR-KLGR modified YSK05-MEND in LSEC increased with an increase in the amount of STR-KLGR at on the YSK05-MEND. There is complete shift in fluorescence intensity with an increase in the modification rate of the MEND (Fig. 3A). When cellular uptake was plotted as a function of mean fluorescence, the plot showed a gradual increase in the cellular uptake with an increase in ligand at the surface of MEND (Fig. 3B). These data completely supports the in vivo results. Comparing the cellular accumulation and gene expression data (Figs. 1 and 2) it appears that the knockdown of gene expression is at a maximum when the surface modification of YSK05-MEND by STR-KLGR is at a minimum, for example 1 mol%. We then checked the knockdown efficiency of the YSK05-MEND when the ligand density at the MEND surface is lower than 1 mol%, for example 0.1 mol% or 0.5 mol%.

3.5. Effect of low density of STR-KLGR at YSK05-MEND in in vivo gene expression

We performed this study to compare the effect of low amounts of STR-KLGR with high amounts of STR-KLGR at the YSK05-MEND surface. In this study, we considered 1 mol% of STR-KLGR to represent a high density of ligand as it showed the maximum knockdown effect of Tie2 gene expression (Fig. 4). As a low density of ligand, we compared 0.1 mol% and 0.5 mol% of STR-KLGR. As KLGR is a highly cationic peptide, we also compared a STR-KLGR modified YSK05-MEND with STR-R8 modified YSK05-MEND. The data showed that 0.5 mol% of STR-KLGR modified YSK05-MEND showed a better knocking down of the Tie2 gene expression than 1 mol% STR-KLGR modified YSK05-MEND (Fig. 4). It also showed a better knockdown efficiency than that of the STR-R8 modified YSK05-MEND.

3.6. Selectivity of the STR-KLGR modified YSK05-MEND for LSEC

This purpose of this experiment was to evaluate the selectivity of our developed carrier for either LSEC or hepatocytes. For this purpose, we observed the knockdown of Tie2 gene expression in

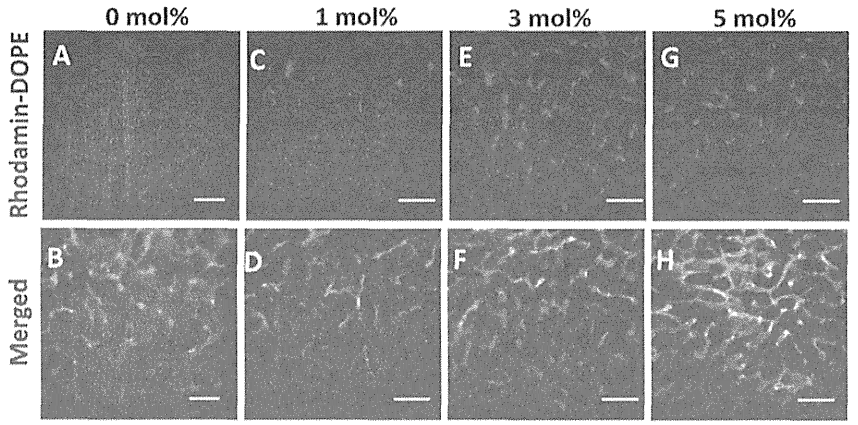

Fig. 2. In vivo accumulation of YSK05-MEND modified with 0 mol% (A and B), 1 mol% (C and D), 3 mol% (E and F) and 5 mol% (G and H) of STR-KLGR. Green and red color represents blood vessels stained with Isolectin B4 and rhodamine-DOPE labeled MEND, respectively. Scale bars correspond to 50 μm in all images. (For interpretation of the references to color in this figure legend, the reader is referred to the web version of this article.)

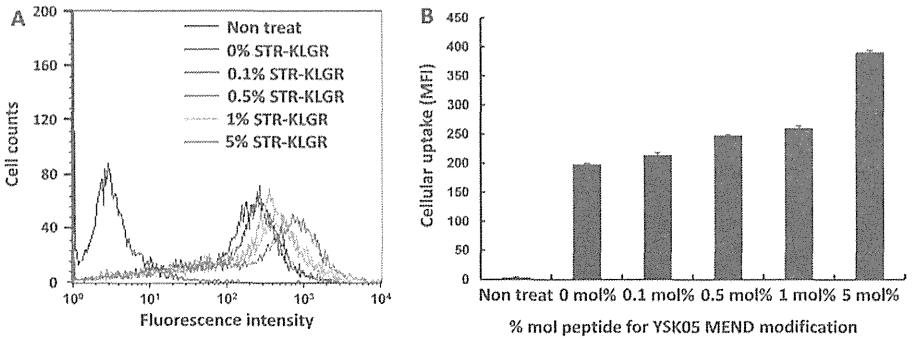

Fig. 3. In vitro cellular uptake study by flow cytometry. (A) Fluorescence intensity of NBD-DOPE labeled YSK05-MEND modified with different mol% of STR-KLGR and (B) mean fluorescence intensity (MFI) of STR-KLGR modified NBD-DOPE labeled YSK05-MEND by LSECs, where $n = 3$.

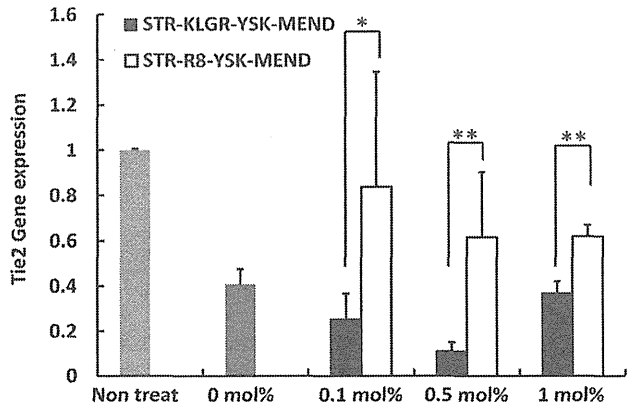

Fig. 4. In vivo Tie2 gene expression by YSK05-MEND modified with low density of STR-KLGR or STR-R8 at the MEND surface. Male ICR mice were intravenously injected with YSK05-MEND modified with different mol% of STR-KLGR or STR-R8 encapsulating Tie2 siRNA in the core. Liver samples were collected after 24 h of incubation. After collecting mRNA from the liver samples, Tie2 gene expression level was measured by RT-PCR. Number of mouse in each sample group = 5. Statistical analysis within each groups was done by unpaired t-test, where $^{**}P < 0.01$ and $^{*}P < 0.05$.

LSEC and FVII expression in hepatocytes. Tie2 was already identified as a receptor tyrosine kinase that is expressed principally on the vascular endothelium (Peters et al., 2004). It has been also reported that all the coagulation factors are produced by the liver and among these coagulation factors, hepatocytes produce the FVII factor (Cronin et al., 2012). We delivered

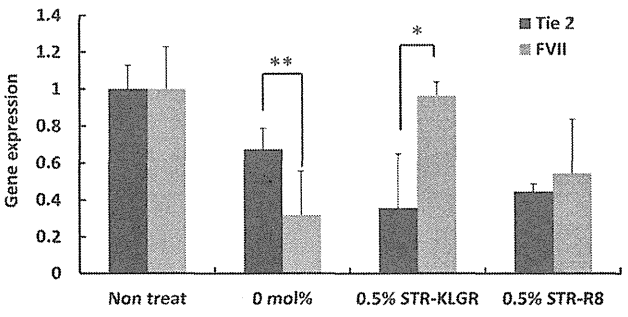

Fig. 5. In vivo Tie2 and FVII gene expression by YSK05-MEND modified with 0.5 mol % of STR-KLGR or STR-R8 at the MEND surface. Male ICR mice were intravenously injected with YSK05-MEND modified with different mol% of STR-KLGR or STR-R8 encapsulating either Tie2 siRNA or FVII siRNA. After 24 h of incubation, liver samples were collected. After collecting mRNA from the liver samples, Tie2 or FVII gene expression levels were measured by RT-PCR. Number of mice in each sample group = 4. Statistical analysis within each groups was done by unpaired t-test, where $^{**}P < 0.01$ and $^{*}P < 0.05$.

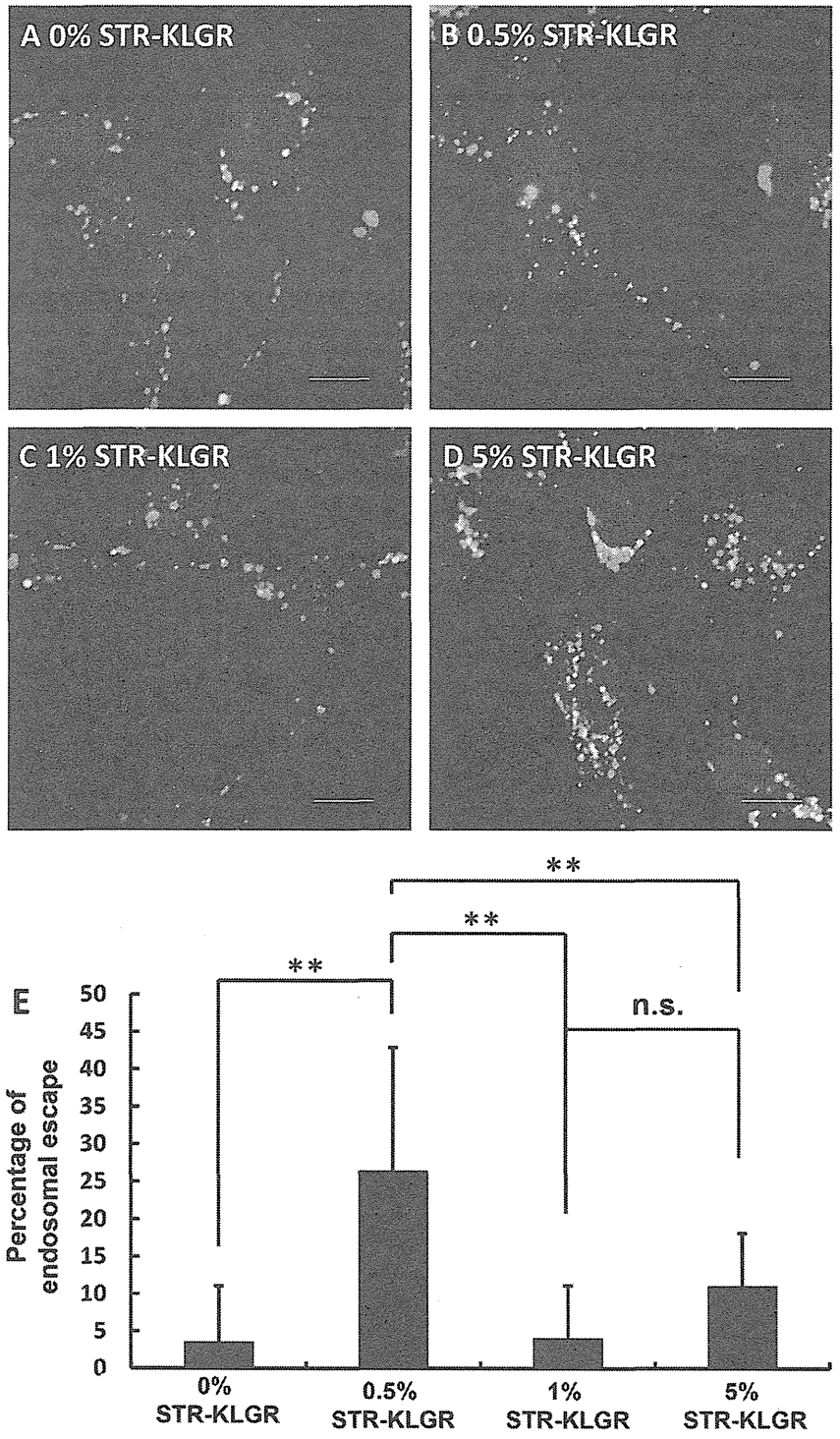

Fig. 6. Endosomal escape efficiency of YSK05-MEND modified with (A) 0 mol%, (B) 0.5 mol%, (C) 1 mol% and (D) 5 mol%. MEND encapsulating cy3-labeled Tie 2 siRNA were transfected into LSECs. The endosomes/lysosomes (green) were stained with Lysotracker green to differentiate between siRNA in endosomes/lysosomes (yellow) and the cytosol (red). The fraction of siRNA in endosomes and the cytosol was quantified based on the pixel area of clusters in each region of interest, as described in Section 2.11. (E) Quantitative comparison of endosome escape efficiency between each group where endosome escape efficiency in 10 individual cells was plotted. Red bars represent the average values. Statistical differences between groups were evaluated by ANOVA followed by SNK test where $^{**}P < 0.01$, n.s. = not significant. Scale bars correspond to 50 μm in all images. (For interpretation of the references to color in this figure legend, the reader is referred to the web version of this article.)

Tie2 siRNA or FVII siRNA using either the modified or unmodified YSK05-MEND to lower the gene expression of endothelial cell specific marker Tie2 gene or hepatocyte specific FVII factor respectively. The result showed that the YSK05-MEND modified with 0.5 mol% STR-KLGR successfully lowered Tie2 gene expression than FVII gene expression and the difference was statistically significant (Fig. 5). We also compared the result with the knockdown efficiency of the STR-R8 modified YSK05-MEND. It shows that the STR-R8 modified YSK05-MEND caused a similar lowering of gene expression in both genes.

3.7. Endosomal escape efficiency of STR-KLGR modified YSK05-MEND in LSEC

To evaluate the effect of different modification rates for STR-KLGR on the YSK05-MEND on intracellular trafficking efficiency, in vitro endosomal escape efficiency was measured by evaluating confocal microscopic images (Fig. 6A–D). When we plotted the pixel count of 10 different cells in each group, the results indicated that the endosomal escape efficiency was at a maximum when the amount of ligand at the MEND surface was at a minimum (Fig. 6E). Endosomal escape efficiency is highest for a 0.5 mol% of modification with STR-KLGR at the nano carrier surface while at a concentration of 1 mol% or 5 mol% of STR-KLGR, the endosomal escape efficiency of cy3 labeled Tie2 siRNA was decreased and the difference was statistically significant (Fig. 6E).

3.8. Uptake mechanism study by confocal microscope

An in vitro cellular uptake mechanism study was performed to determine the intracellular fate of both modified and unmodified YSK05-MEND used for siRNA delivery in both LSEC and a Hepa1–6 line. In this experiment, different inhibitors were used to inhibit different uptake pathways. It has been reported that Amiloride inhibits macropinocytosis by inhibiting the Na^+/H^+ exchange required for macropinocytosis (Hewlett et al., 1994), a hypertonic sucrose solution inhibits clathrin-mediated endocytosis via dissociation of the clathrin lattice (Heuser and Anderson, 1989) and Filipin III inhibits caveolar uptake through cholesterol depletion (Lamaze and Schmid, 1995). The results of this experiment are summarized in Table 2. As shown in figure, the unmodified YSK05-MEND follows both macropinocytosis and clathrin-mediated endocytosis in LSEC (Fig. 7a) as well as in the Hepa 1–6 cell line (Fig. 7b). It is interesting to note that Fillipin III increased the cellular uptake of the MEND in LSEC to a significant extent (Fig. 7a C,G and K).

A possible explanation for this may be morphological changes caused by the Filipin III treatment. A previous report also indicated such a phenomenon in urothelial cells when they were incubated with Filipin III (Berry et al., 2009). Some data are presented here which indicates that in some cells, filipin may have increased intracellular trafficking by modifying cell morphology. When the YSK05-MEND is modified with 0.5 mol% of STR-KLGR then in LSEC, it is following macropinocytosis or clathrin-mediated endocytosis in LSEC but in Hepa1–6 cell line it is following only clathrin-mediated endocytosis. The YSK05-MEND follows only clathrin-mediated endocytosis regardless of cell type when the surface of the MEND is modified with a higher density of ligand which is 5 mol%.

4. Discussion

The goal of this study was to develop a new LSEC targeted nanocarrier for delivering siRNA to LSEC in a manner that can successfully avoid lysosomal degradation and can achieve successful down regulation of an endothelial cell specific gene. Though there are several approaches for gene delivery to the liver, a very few of them can be utilized to target LSEC. Moreover, although some carriers can target LSEC specifically but ultimately fails to deliver a gene to the cell cytosol (Bartsch et al., 2004).

In this experiment, an attempt was made to prepare a nanocarrier that is selective for LSEC. Here, YSK05-MEND was used as a carrier for siRNA delivery. YSK05-MEND was previously reported from our lab. This MEND is made from a cationic lipid YSK05 which has fusogenic properties. The YSK05-MEND was reported to have a higher ability for endosomal escape than other MENDs containing conventional cationic lipids (Sato et al., 2012). For modifying the surface of the MEND with an LSEC specific ligand we used the KLGR peptide, which has been previously reported by our group (Akhter et al., 2013). The KLGR-PEG modified liposomal system showed a high selectivity for LSEC (Akhter et al., 2013). Because of this, in this study, the surface of the YSK05-MEND was modified with KLGR-PEG. But PEG_{2000}-DSPE was used as a PEG linker in this study. This type of PEG linker has some drawbacks in terms of endosomal escape efficiency. The major criteria for better endosomal escape efficiency is the fusion of the lipid bilayer of a liposome or MEND with the endosomal lipid bilayer which will ultimately release the core material of the MEND into the cytosol (Hatakeyama et al., 2011). However, some PEG-linkers can inhibit the fusogenic property of the MEND. For successful fusion, first, the PEG should be shed from the lipid bilayer of MEND (Hatakeyama et al., 2011). But in case of PEG_{2000}-DSPE, the double hydrocarbon chain of DSPE is attached to the lipid bilayer so tightly that it becomes impossible to shed the PEG. This phenomenon was referred to as the PEG-dilemma in a previous study (Hatakeyama et al., 2011). One previous report showed that the introduction of stearylated octaarginine (STR-R8) into the lipid envelope (R8-MEND) enhanced the cellular uptake of the MEND (Kogure et al., 2007). As an advance remedy for the PEG dilemma, we planned to introduce STR-KLGR as a modifier for the YSK05-MEND.

The in vivo gene knockdown experiment showed that KLGR-PEG modified MEND could not achieve the desired suppression of gene expression and we attribute this to the effect of the PEG-

Table 2
Summary of the uptake pathway.

MEND	Uptake pathway	
	LSEC	Hepatocyte
Unmodified	1. Macropinocytosis 2. Clathrin mediated endocytosis	1. Macropinocytosis 2. Clathrin mediated endocytosis
0.5 mol% KLGR	1. Macropinocytosis 2. Clathrin mediated endocytosis	1. Clathrin mediated endocytosis
5 mol% KLGR	1. Clathrin mediated endocytosis	1. Clathrin mediated endocytosis

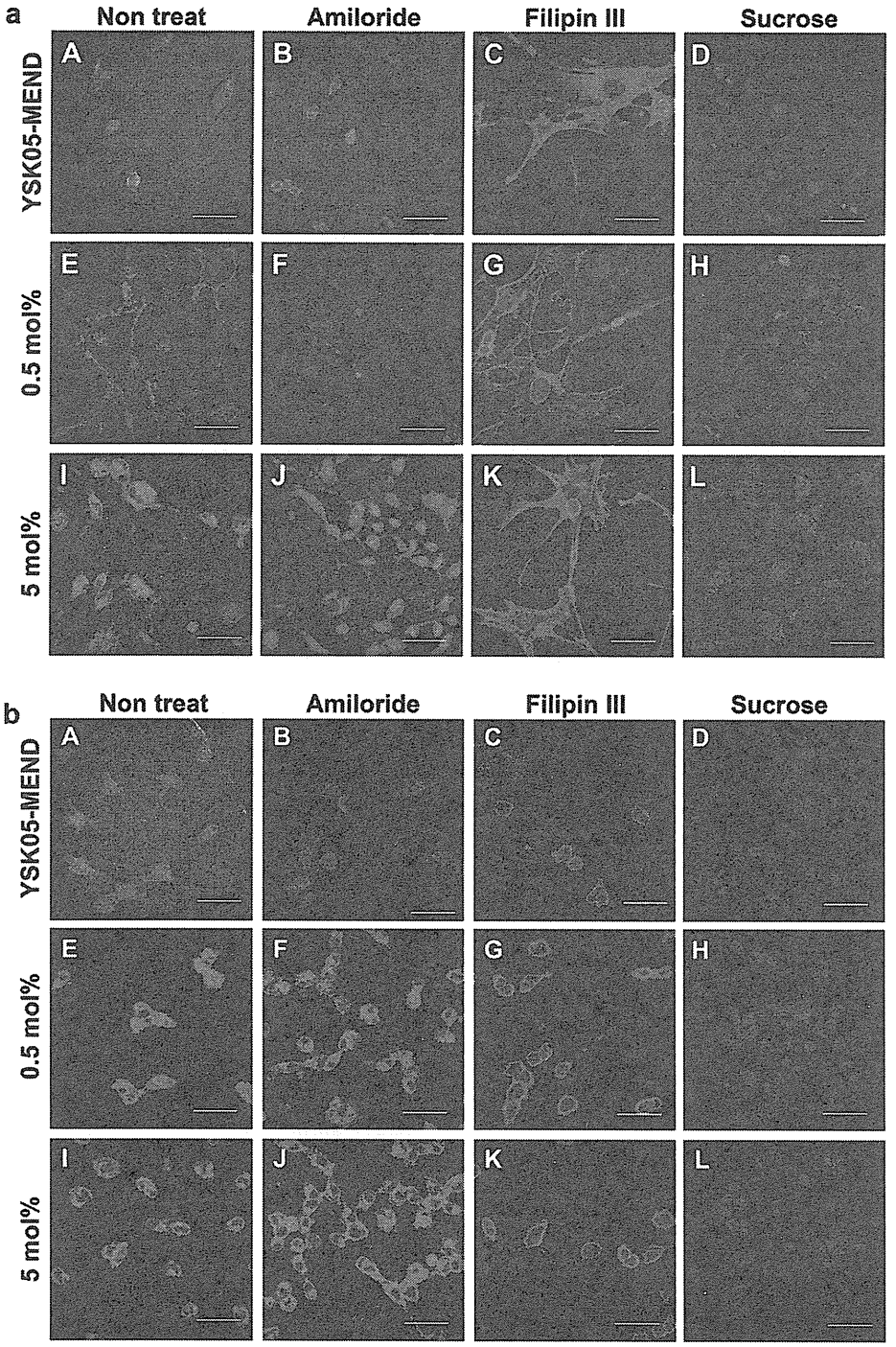

Fig. 7. (a) In vitro uptake mechanism of rhodamin-DOPE labeled YSK05-MEND modified with (A–D) 0 mol%, (E–H) 0.5 mol%, and (I–L) 5 mol% in LSECs in presence or absence of three inhibitor amiloride, Filipin III and hypertonic sucrose in LSEC. Here, red denotes the rhodamin-DOPE labeled MEND and blue represents the nucleus stained with Hoechst 33342. Scale bars correspond to 50 μm in all images. (b) In vitro uptake mechanism of rhodamin-DOPE labeled YSK05-MEND modified with (A–D) 0 mol%, (E–H) 0.5 mol%, and (I–L) 5 mol% in Hepa1–6 cell line in presence or absence of three inhibitor amiloride, Filipin III and hypertonic sucrose in Hepa1–6 cell line. Here, red denotes the rhodamin-DOPE labeled MEND and blue represents the nucleus stained with Hoechst 33342. Scale bars correspond to 50 μm in all images. (For interpretation of the references to color in this figure legend, the reader is referred to the web version of this article.)

dilemma. However, the STR-KLGR modified MEND achieved an 80% knockdown of Tie2 gene expression (Fig. 1). It is notable that gene expression silencing activity increased with decreasing amounts of STR-KLGR at the surface of the YSK05-MEND. To verify the uptake of the developed carrier, we decided to carry out an in vivo accumulation study by confocal microscopy. The in vivo confocal study showed that the uptake of modified MEND increased with increasing amounts of surface ligand (Fig. 2). Here, the YSK05-MEND modified with 0 mol% of STR-KLGR showed the least accumulation through the blood vessel (Fig. 2A and B) and modification with 5 mol% STR-KLGR

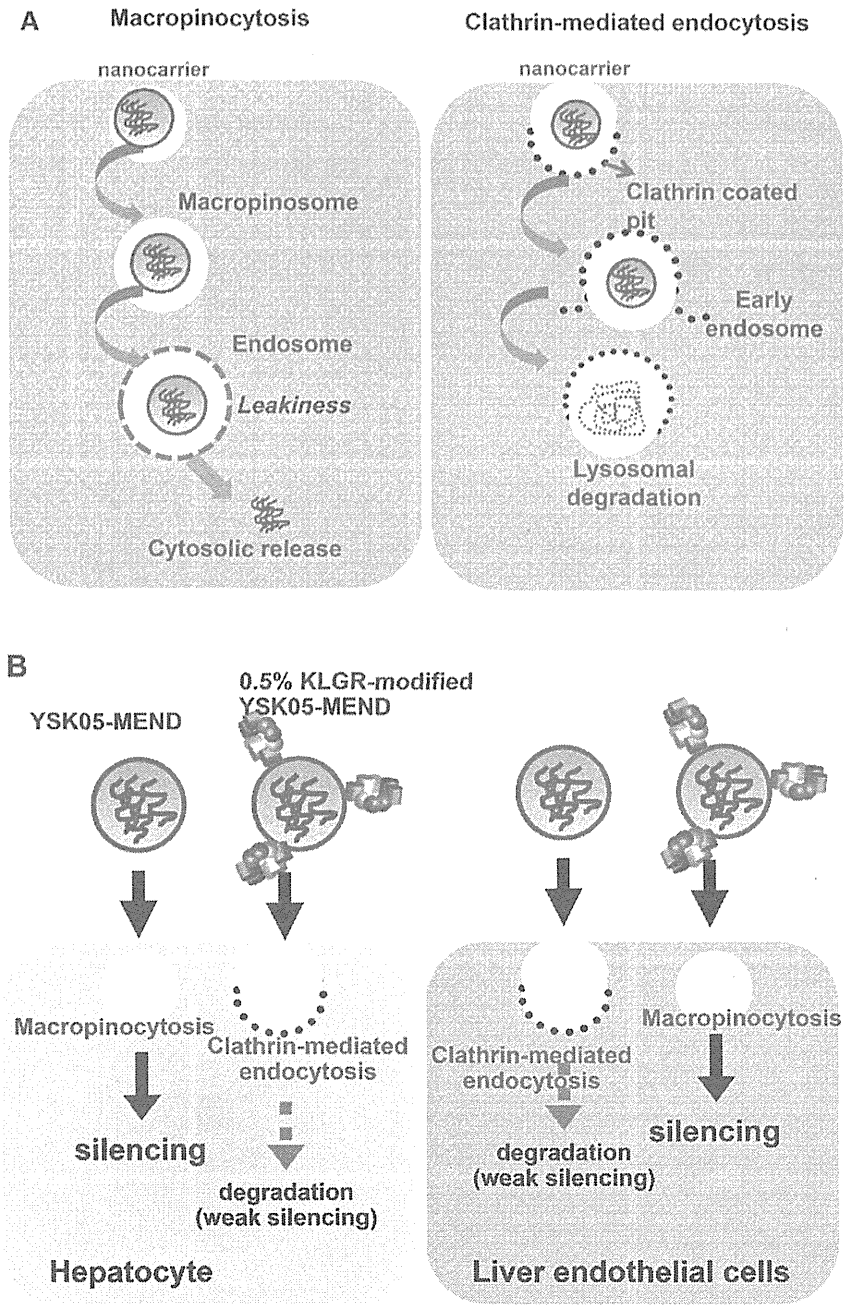

Fig. 8. Graphical representation of the mechanism responsible for the uptake of the YSK05-MEND. (A) Macropinocytosis and clathrin-mediated endocytosis lead to an effective silencing and lysomal degradation, respectively. (B) YSK05-MEND and the ligand-modified YSK05-MEND would be taken up by each uptake pathway via hepatocytes and LSECs.

showed the most (Fig. 2G and H). An uptake study with flow cytometry also supported these findings (Fig. 3A and B). Further, gene silencing experiment with YSK05-MEND modified with lower amounts of STR-KLGR such as 0.5 mol% or 0.1 mol% showed that 0.5 mol% STR-KLGR modified YSK05-MEND resulted in the maximum knockdown efficiency (Fig. 4). These data indicates that for better siRNA delivery to LSEC, the first criterion is to optimize the amount of ligand used to modify the carrier.

For describing these reverse relationships between accumulation and gene silencing activity, we attempted to observe the endosomal escape efficiency of the STR-KLGR modified YSK05-MEND. This result showed that the YSK05-MEND modified with a lower amount of STR-KLGR, i.e., 0.5 mol% permits a more efficient escape from endosomes than a 1 mol% or 5 mol% modifications. This result can explain the reverse relationship between cellular uptake and gene silencing activity. As can be seen in the confocal image of the endosomal escape efficiency experiment, a 5 mol% modification shows a more merged signal of cy3 labeled siRNA with the acidic endosomal compartment in the cytosol than a 0.5 mol% modification suggesting that endosomal entrapment for the 5 mol% STR-KLGR modified YSK05-MEND is greater than other modifications (Fig. 6A–D). Graphical presentation of the pixel count of red and yellow areas in the confocal microscopic image showed that endosomal escape is highest for 0.5 mol% KLGR-PEG than 1 mol% or 5 mol% STR-KLGR modified YSK05-MEND

(Fig. 6E). This result explains the reason behind the lower knockdown of gene expression at higher modification of ligand. Probably the low endosomal escape capacity of 5 mol% STR-KLGR modified YSK05-MEND reduces the ability of the MEND to release siRNA into the cell cytoplasm. Therefore, 0.5 mol% STR-KLGR-modified YSK05-MEND was able to allow the successful delivery of siRNA to LSEC. This carrier was more selective to LSEC rather than hepatocytes, since 0.5 mol% STR-KLGR-modified YSK05-MEND showed a better gene expression knockdown efficiency in LSEC than hepatocytes and the difference was statistically significant, while the 0.5 mol% STR-R8 modified YSK05-MEND showed a similar gene expression knockdown efficiency in both LSEC and hepatocytes (Fig. 5). Evaluation of the uptake mechanism would be expected to reveal the reason for this selective siRNA delivery of 0.5 mol% STR-KLGR modified YSK05-MEND to LSEC.

The uptake mechanism study shows that unmodified YSK05-MEND is internalized into the cell via macropinocytosis and clathrin-mediated endocytosis, in both LSEC (Fig. 7a A–D) and a Hepa1–6 cell line (Fig. 7b A–D). When the surface ligand density is low (0.5 mol%), the carrier is then internalized into LSEC by both macropinocytosis and clathrin-mediated endocytosis (Fig. 7a E–H) but only clathrin-mediated endocytosis is operative in the case of Hepa1–6 (Fig. 7b E–H). However, when the ligand density is higher, clathrin-mediated endocytosis occurs (Fig. 7a I–L and b I–L). As clathrin-mediated endocytosis is susceptible to lysosomal degradation (McMahon and Boucrot, 2011) (Fig. 8, right) so the YSK05-MEND containing a high density of ligand at its surface fails to deliver siRNA regardless of cell type. At a low density of ligand, the modified YSK05-MEND follows macropinocytosis in LSEC which is less susceptible to lysosomal degradation (Yu et al., 2012) (Fig. 8A left) and was previously reported to be involved in the delivery of siRNA to the cell cytosol (Gilleron et al., 2013) but in hepatocytes it is taken up via clathrin-mediated endocytosis (Fig. 8B). This is a possible cause for the successful knockdown of gene expression in LSEC, compared to hepatocytes (Fig. 5) by the YSK05-MEND that was modified with 0.5 mol% STR-KLGR. While the unmodified YSK05-MEND follows macropinocytosis in both types of cells, no specificity for any of the cells was observed (Fig. 5). Above all, 0.5 mol% STR-KLGR modified YSK05-MEND successfully targets LSEC and can deliver siRNA to the cell cytosol, thus, avoiding lysosomal degradation, which results in an acceptable knockdown efficiency of endothelial cell specific Tie2 gene expression. However, further experiments to observe the cell selectivity of our developed MEND showed moderate selectivity for liver endothelilal cells rather than endothelial cells in lungs or the kidney (Supplementary Fig. 1). The safety of this system was comparable to non treated mice (Supplementary Fig. 2). Considering all these data, it can be assumed that the developed STR-KLGR modified YSK05-MEND has the potential for serving as an effective tool for gene therapy targeting LSEC.

5. Conclusion

For developing a successful targeted gene carrier for targeting LSEC for siRNA therapy, three basic parameters should be considered, namely ligand density at the nanocarrier surface, endosomal escape efficiency and the mechanism responsible for the uptake of the carrier by the targeted cells. Considering these three points, STR-KLGR modified YSK05-MEND successfully met all the three of these criteria, allowing us to conclude that this delivery system is deserving of further study, to suppress disease related genes in LSECs.

Acknowledgements

This study was supported by grants from the Special Education and Research Expenses of the Ministry of Education, Culture, Sports, Science and Technology of Japan. The authors also wish to thank Dr. Milton S. Feather for his helpful advice in writing the English manuscript.

Appendix A. Supplementary data

Supplementary data associated with this article can be found, in the online version, at http://dx.doi.org/10.1016/j.ijpharm.2014.08.048.

References

Akhter, A., Hayashi, Y., Sakurai, Y., Ohga, N., Hida, K., Harashima, H., 2013. A liposomal delivery system that targets liver endothelial cells based on a new peptide motif present in the ApoB-100 sequence. Int. J. Pharm. 456, 195–201.
Akino, T., Hida, K., Hida, Y., Tsuchiya, K., Freedman, D., Muraki, C., 2009. Cytogenetic abnormalities of tumor-associated endothelial cells in human malignant tumors. Am. J. Pathol. 75, 2657–2667.
Bartsch, M., Weeke-Klimp, A.H., Hoenselaar, E.P., Stuart, M.C., Meijer, D.K., Scherphof, G.L., Kamps, J.A., 2004. Stabilized lipid coated lipoplexes for the delivery of antisense oligonucleotides to liver endothelial cells in vitro and in vivo. J. Drug Target. 12, 613–621.
Berry, R.E., Klumpp, D.J., Schaeffer, A.J., 2009. Urothelial cultures support intracellular bacterial community formation by uropathogenic *Escherichia coli*. Infect. Immun. 77, 2762–2772.
Cronin, K.R., Mangan, T.P., Carew, J.A., 2012. Upregulation of the coagulation factor VII gene during glucose deprivation is mediated by activating transcription factor 4. PLoS One 7, e40994.
DeLeve, L.D., 2011. Vascular Liver Disease: Mechanisms and Management. Springer Science & Business Media, pp. 25–40.
Gilleron, J., Querbes, W., Zeigerer, A., Borodovsky, A., 2013. Image-based analysis of lipid nanoparticle-mediated siRNA delivery, intracellular trafficking and endosomal escape. Nat. Biotechnol. 31, 638–646.
Hatakeyama, H., Akita, H., Harashima, H., 2011. A multifunctional envelope type nano device (MEND) for gene delivery to tumours based on the EPR effect: a strategy for overcoming the PEG dilemma. Adv. Drug Deliv. Rev. 63, 152–160.
Hewlett, L.G., Prescott, A.R., Watts, C., 1994. The coated pit and macropinocytic pathways serve distinct endosome populations. J. Cell Biol. 124, 689–703.
Heuser, J.E., Anderson, R.G., 1989. Hypertonic media inhibit receptor-mediated endocytosis by blocking clathrin-coated pit formation. J. Cell Biol. 108, 389–400.
Hida, K., Hida, Y., Amin, D.N., Flint, A.F., Panigrahy, D., Mortonet, C.C., 2004. Tumor-associated endothelial cells with cytogenetic abnormalities. Cancer Res. 64, 8249–8255.
Kren, B.T., Unger, G.M., Sjeklocha, L., Trossen, A.A., Korman, V., Diethelm-Okita, B.M., 2009. Nanocapsule-delivered sleeping beauty mediates therapeutic factor VIII expression in liver sinusoidal endothelial cells of hemophilia a mice. J. Clin. Investig. 119, 2086–2099.
Kogure, K., Akita, H., Harashima, H., 2007. Multifunctional envelope-type nano device for non-viral gene delivery: concept and application of programmed packaging. J. Control. Release 122, 246–251.
Lamaze, C., Schmid, S.L., 1995. The emergence of clathrin-independent pinocytic pathways. Curr. Opin. Cell Biol. 7, 573–580.
McMahon, H.T., Boucrot, E., 2011. Molecular mechanism and physiological functions of clathrin-mediated endocytosis. Nat. Rev. Mol. Cell Biol. 12, 517–533.
March, S., Hui, E.E., Underhill, G.H., Khetani, S., Bhatia, S.N., 2009. Microenvironmental regulation of the sinusoidal endothelial cell phenotype in vitro. Hepatology 50, 920–928.
Neumann, K., Kruse, N., Wechsung, K., 2011. Chemokine presentation by liver sinusoidal endothelial cells as therapeutic target in murine T cell-mediated hepatitis. Z. Gastroenterol. 49, V04.
Neubauer, K., Wilfling, T., Ritzel, A., Ramadori, G., 2000. Platelet-endothelial cell adhesion molecule-1 gene expression in liver sinusoidal endothelial cells during liver injury and repair. J. Hepatol. 32, 921–932.
Ohga, N., Hida, K., Hida, Y., Muraki, C., Tsuchiya, K., Matsuda, K., 2009. Inhibitory effects of epigallocatechin-3 gallate, a polyphenol in green tea, on tumor-associated endothelial cells and endothelial progenitor cells. Cancer Sci. 100, 1963–1970.
Oshita, M., Sato, N., Yoshihara, H., Takei, Y., Hijioka, T., Fukui, H., Goto, M., Matsunaga, T., Kawano, S., Fusamoto, H., 1992. Ethanol-induced vasoconstriction causes focal hepatocellular injury in the isolated perfused rat liver. Hepatology 16, 1007–1013.
Peters, K.G., Kontos, C.D., Lin, P.C., Wong, A.L., Rao, P., Huang, L., Dewhirst, M.W., Sankar, S., 2004. Functional significance of Tie2 signaling in the adult vasculature. Recent Prog. Horm. Res. 59, 51–71.
Ramadori, G., Moriconi, F., Malik, I., Dudas, J., 2008. Physiology and pathophysiology of liver inflammation damage and repair. J. Physiol. Pharmacol. 59, 107–117.
Samantha, Y., Hidekazu, T., Vijay, K.K., 2009. Ethanol-induced expression of ET-1 and ET-BR in liver sinusoidal endothelial cells and human endothelial cells involves hypoxia-inducible factor-1α and microRNA-199. J. Immunol. 5232–5243.
Sakurai, Y., Hatakeyama, H., Sato, Y., Hyodo, M., Akita, H., Harashima, H., 2013. Gene silencing via RNAi and siRNA quantification in tumor tissue using MEND, a liposomal siRNA delivery system. Mol. Ther. 21, 1195–1203.

Sato, Y., Hatakeyama, H., Sakurai, Y., Hyodo, M., Akita, H., Harashima, H., 2012. A pH-sensitive cationic lipid facilitates the delivery of liposomal siRNA and gene silencing activity in vitro and in vivo. J. Control. Release 163, 267–276.

Takei, Y., Maruyama, A., Ferdous, A., Nishimura, Y., 2004. Targeted gene delivery to sinusoidal endothelial cells: DNA nanoassociate bearing hyaluronan-glycocalyx. FASEB J. 18, 699–701.

Toriyabe, N., Hayashi, Y., Harashima, H., 2013. The transfection activity of R8-modified nanoparticles and siRNA condensation using pH sensitive stearylated-octahistidine. Biomaterials 34, 1337–1343.

Urban, O., German, C., Goran, B., 1993. Binding of a synthetic apolipoprotein B-100 peptide and peptide analogues to chondroitin 6-dulfate: effects of the lipid environment. Biochemistry 32, 1858–1865.

Urban, O., German, C., Eva, H.C., Karin, E., Goran, B., 2010. Possible functional interactions of apolipoprotein B-100 segments that associate with cell proteoglycans and the ApoB/E receptor. Arterioscler. Thromb. Vasc. Biol. 17, 149–152.

Yu, B., Hsu, S.H., Zhou, C., Wang, X., Terp, M.C., Wu, Y., Teng, L., 2012. Lipid nanoparticles for hepatic delivery of small interfering RNA. Biomaterials 33, 5924–5934.

Biomaterials 35 (2014) 7110–7120

Contents lists available at ScienceDirect

Biomaterials

journal homepage: www.elsevier.com/locate/biomaterials

An aptamer ligand based liposomal nanocarrier system that targets tumor endothelial cells

Mst. Naznin Ara [a,1], Takashi Matsuda [b,1], Mamoru Hyodo [a], Yu Sakurai [a], Hiroto Hatakeyama [a], Noritaka Ohga [c], Kyoko Hida [c], Hideyoshi Harashima [a,b,*]

[a] Laboratory of Innovative Nanomedicine, Faculty of Pharmaceutical Sciences, Hokkaido University, Kita 12, Nishi 6, Kita-ku, Sapporo, Hokkaido 060-0812, Japan

[b] Laboratory for Molecular Design of Pharmaceutics, Faculty of Pharmaceutical Sciences, Hokkaido University, Kita 12, Nishi 6, Kita-ku, Sapporo, Hokkaido 060-0812, Japan

[c] Division of Vascular Biology, Graduate School of Dental Medicine, Hokkaido University, Kita 13, Nishi 7, Kita-ku, Sapporo, Hokkaido 060-0812, Japan

ARTICLE INFO

Article history:
Received 28 March 2014
Accepted 18 April 2014
Available online 27 May 2014

Keywords:
Targeted delivery
Aptamer-liposomes
Endocytosis
Intracellular uptake
Tumor endothelial cells

ABSTRACT

The objective of this study was to construct our recently developed aptamer-modified targeted liposome nano-carrier (Apt-PEG-LPs) system to target primary cultured mouse tumor endothelial cells (mTEC), both *in vitro* and *in vivo*. We first synthesized an aptamer-polyethylene glycol 2000-distearoyl phosphoethanolamine (Apt-PEG_{2000}-DSPE). The conjugation of the Apt-PEG_{2000}-DSPE was confirmed by MALDI-TOF mass spectroscopy. A lipid hydration method was used to prepare Apt-PEG-LPs, in which the outer surface of the PEG-spacer was decorated with the aptamer. Apt-PEG-LPs were significantly taken up by mTECs. Cellular uptake capacity was observed both quantitatively and qualitatively using spectrofluorometry, and confocal laser scanning microscopy (CLSM), respectively. In examining the extent of localization of aptamer-modified liposomes that entered the cells, approximately 39% of the Apt-PEG-LPs were not co-localized with lysotracker, indicating that they had escaped from endosomes. The uptake route involved a receptor mediated pathway, followed by clathrin mediated endocytosis. This Apt-PEG-LP was also applied for *in vivo* research whether this system could target tumor endothelial cells. Apt-PEG-LP and PEG_{5000}-DSPE modified Apt-PEG-LP (Apt/PEG_{5000}-LP) were investigated by human renal cell carcinoma (OS-RC-2 cells) inoculating mice using CLSM. Apt-PEG-LP and Apt/PEG_{5000}-LP showed higher accumulation on tumor vasculature compared to PEG-LP and the co-localization efficacy of Apt-PEG-LP and Apt/PEG_{5000}-LP on TEC were quantified 16% and 25% respectively, which was also better than PEG-LP (3%). The findings suggest that this system is considerable promise for targeting tumor endotheiial cells to deliver drugs or genes *in vitro* and *in vivo*.

1. Introduction

A continuous affordable, but still greater challenge remains in nano-medicine in terms of cancer diagnosis, and therapy designed to deliver imaging agents or chemotherapeutic drugs to cells in a specific and selective manner [1]. The successful delivery of cytotoxic drugs via passive or active targeting is an important issue in the design and construction of new and improved targeting drug delivery systems. Small molecules such as peptides, as well as antibodies have been widely used targeting agents, and has enjoyed some (but not sufficient) success, when incorporated with nano-materials. The resulting constructs are often dictated more by the materials used rather than the targeting agents. Researchers are currently attempting to develop more and more new types of therapy [2–5]. To meet these challenges, nucleic acid aptamers are now of great interest as new targeting small molecules. Aptamers are single stranded oligonucleotides, ssDNA or ssRNA molecules produced by SELEX [6,7]. Cell-SELEX is a modified selection method against live cells [8]. Aptamers are very easy to reproduce, are low in cost, generally nontoxic, and have a low molecular weight (8–15 kDa). This single stranded DNA or RNA oligonucleotide can fold into well-defined 3D structures and bind to their target with a high affinity (μM to pM range) and specificity [9,10].

* Corresponding author. Faculty of Pharmaceutical Sciences, Hokkaido University, Kita-12, Nishi-6, Kita-ku, Sapporo, Hokkaido 060-0812, Japan. Tel.: +81 11 706 2197; fax: +81 11 706 4879.
E-mail address: harasima@pharm.hokudai.ac.jp (H. Harashima).

[1] Those authors were equally contributed.

http://dx.doi.org/10.1016/j.biomaterials.2014.04.087
0142-9612/